

RESEARCH

Open Access



# Enhancement of PD-L1-attenuated CAR-T cell function through breast cancer-associated fibroblasts-derived IL-6 signaling via STAT3/AKT pathways

Nisa Chuangchot<sup>1,2</sup>, Pranisa Jamjuntra<sup>1</sup>, Supaporn Yangngam<sup>1</sup>, Piriya Luangwattananun<sup>2,3</sup>,  
Suyanee Thongchot<sup>1,2</sup>, Mutita Junking<sup>2,3</sup>, Peti Thuwajit<sup>1</sup>, Pa-Thai Yenchitsomanus<sup>2,3</sup> and Chanitra Thuwajit<sup>1\*</sup>

## Abstract

**Background** Carcinoma-associated fibroblasts (CAFs) play a critical role in cancer progression and immune cell modulation. In this study, it was aimed to evaluate the roles of CAFs-derived IL-6 in doxorubicin (Dox) resistance and PD-L1-mediated chimeric antigenic receptor (CAR)-T cell resistance in breast cancer (BCA).

**Methods** CAF conditioned-media (CM) were collected, and the IL-6 level was measured by ELISA. CAF-CM were treated in MDA-MB-231 and HCC70 TNBC cell lines and *siIL-6* receptor (IL-6R) knocked down (KD) cells to determine the effect of CAF-derived IL-6 on Dox resistance by flow cytometry and on increased PD-L1 through STAT3, AKT and ERK1/2 pathways by Western blot analysis. After pre-treating with CM, the folate receptor alpha (FR $\alpha$ )-CART cell cytotoxicity was evaluated in 2D and 3D spheroid culture assays.

**Results** The results showed a significant level of IL-6 in CAF-CM compared to that of normal fibroblasts (NFs). The CM with high IL-6 level significantly induced Dox resistance; and PD-L1 expression through STAT3 and AKT pathways in MDA-MB-231 and HCC70 cells. These induction effects were attenuated in *siIL-6R* KD cells. Moreover, the TNBC cell lines that were CM-treated with STAT3 and an AKT inhibitor had a reduced effect of IL-6 on PD-L1 expression. BCA cells with high IL-6 containing-CM treatment had resistance to cancer cell killing by FR $\alpha$  CAR-T cells compared to untreated cells.

**Conclusion** These results highlight CAF-derived IL-6 in the resistance of chemotherapy and T cell therapy. Using inhibitors of IL-6-STAT3/AKT-PD-L1 axis may provide a potential benefit of Dox and CAR-T cell therapies in BCA patients.

**Keywords** Cancer-associated fibroblast, IL-6, PD-L1, Folate receptor- $\alpha$ , CAR-T cell, Doxorubicin

\*Correspondence:

Chanitra Thuwajit

cthuwajit@yahoo.com

Full list of author information is available at the end of the article



© The Author(s) 2023. **Open Access** This article is licensed under a Creative Commons Attribution 4.0 International License, which permits use, sharing, adaptation, distribution and reproduction in any medium or format, as long as you give appropriate credit to the original author(s) and the source, provide a link to the Creative Commons licence, and indicate if changes were made. The images or other third party material in this article are included in the article's Creative Commons licence, unless indicated otherwise in a credit line to the material. If material is not included in the article's Creative Commons licence and your intended use is not permitted by statutory regulation or exceeds the permitted use, you will need to obtain permission directly from the copyright holder. To view a copy of this licence, visit <http://creativecommons.org/licenses/by/4.0/>. The Creative Commons Public Domain Dedication waiver (<http://creativecommons.org/publicdomain/zero/1.0/>) applies to the data made available in this article, unless otherwise stated in a credit line to the data.

## Introduction

Breast cancer (BCA) is the most common cancer of women worldwide [1]. The 2020 global cancer statistics estimate 2.3 million new cases in women [2]. BCA is clustered into four subtypes, including Luminal A, Luminal B, HER2-positive, and triple-negative BCA (TNBC) [3]. Although increased early screening and understanding of molecular mechanisms of metastasis leads to more effective prognosis and treatment, some patients have relapses and chemoresistance, especially in the TNBC [4].

The tumor microenvironment (TME) consists of tumor cells, cancer-associated fibroblasts (CAFs), endothelial cells, extracellular matrix, and immune cells [5]. CAFs, the most abundant cells in TME, secrete substances such as transforming growth factor- $\beta$  (TGF- $\beta$ ), vascular endothelial growth factor (VEGF), and interleukin-6 (IL-6) which can promote cancer progression [6–9]. CAF-derived substances regulate epithelial-mesenchymal transition and promote drug resistance by secreting IL-6 [10, 11]. In addition, fibroblast activation protein (FAP)  $\alpha$ 1-positive CAFs drive immunosuppression [12–14]. These facts declare the importance to investigate CAF-mediated immunosuppression and the involved mechanisms.

IL-6 is released by various cells including cancer cells, CAFs, and immune cells [15]. IL-6/IL-6 receptor (IL-6R) interaction activates Janus kinase (JAK) tyrosine kinases leading to phosphorylating the signal transducer and activator of transcription 3 (STAT3) [15]. This interaction can phosphorylate mitogen-activated protein kinases (MAPK)/ERK leading to enhance cell growth [16]. The phosphoinositol-3 kinase (PI3K)/AKT pathway is induced by IL-6 following JAK phosphorylation. The PI3K/AKT phosphorylation induces gene expression by activating NF- $\kappa$ B to promote anti-apoptosis [17, 18].

Programmed death ligand 1 (PD-L1), the ligand for programmed death 1 (PD-1), is overexpressed in cancer cells after being induced by cytokines [19]. PD-L1 expression in cancer cells leads to immune escape, drug resistance, and cancer metastasis [20]. The PD-L1/PD-1 interaction attenuates T cell function via T cell apoptosis [21]. Patient-derived hepatocellular carcinoma (HCC)-CAFs secrete IL-6 which induces PD-L1 expression on neutrophils via the STAT3 pathway [22]. The PD-1/PD-L1 immune checkpoint inhibitor was approved by the US Food and Drug Administration (FDA) to treat advanced TNBC tumor-expressed PD-L1 [23]. Immunoregulatory roles of CAF-derived IL-6 in promoting drug resistance and inducing T cell dysfunction through IL-6-mediated PD-L1 expression have not been well-addressed in BCA.

In this study, the IL-6 ELISA assay of BCA-derived CAFs was performed to identify IL-6 levels as a major

component in CAFs. The roles of IL-6 signaling to exert doxorubicin (Dox) resistance and response to folate receptor (FR) $\alpha$ -chimeric antigen receptor (CAR)-T cell killing actions were evaluated in parental and IL-6R-transient knocked down TNBC cell lines, with or without specific inhibitors against signaling molecules. The findings highlight the role of CAFs-derived IL-6 in mediating Dox resistance in MDA-MB-231 and HCC70 TNBC cell lines. It can also reduce FR $\alpha$ -CAR T cell function via the upregulation of PD-L1 through the STAT3/AKT pathway. Interestingly, using either blocking IL-6/IL-6R signaling or PD-1/PDL1 inhibitors may serve as a therapeutic target for sensitizing cancer cells to CAR-T cell treatment and restoring BCA cells to Dox treatment.

## Materials and methods

### Cell culture

MDA-MB-231 and HCC70 cells from ATCC (Manassas, VA) were genetically engineered to express mWasabi-luciferase protein [24]. The Lenti-X<sup>TM</sup>-293T cells were from Takara Bio (Takara Bio, San Jose, CA). Lenti-X<sup>TM</sup>-293T and MDA-MB-231 were maintained in DMEM (Gibco; Thermo Fisher Scientific, MA), while HCC70 was cultured in RPMI1640 (Gibco). CAFs were isolated from BCA patients following the protocol approved by Siriraj Institutional Review Board (COA no. Si 329/2017). CAFs and normal fibroblasts (NFs) [normal breast fibroblast (BNF) and human dermal fibroblast (HDF)] were cultured in DMEM/F12 (Gibco). All complete media was supplemented with 10% fetal bovine serum (FBS; Gibco) and 1% penicillin–streptomycin (Sigma-Aldrich, MA) and incubated with cells at 37°C with 5% CO<sub>2</sub>.

### Immunocytochemistry staining for fibroblast markers

Cells were incubated with anti-panCK (1:200, sc-8018; Santa Cruz, CA), anti-VIM (1:500, sc-6260; Santa Cruz), anti-ASMA (1:200, A5228; Sigma, MA), and anti-FAP (1:100, ab53066; Abcam, Cambridge, UK) at RT for 3 h. The anti-mouse IgG-Cy3 (1:2,000, 115-166-071; Jackson ImmunoResearch Laboratories, PA) or anti-rabbit IgG-FITC (1:2,000, ab6717; Abcam) was applied at RT for 1 h. The anti-CD10-FITC (1:5, 21270103; Invitrogen, Thermo Fisher Scientific, MA) and anti-GPR77 (1:30, 342402; Biolegend, CA) were incubated with cells at 4°C overnight. The nuclei were stained with Hoechst dye (1:1,000; Invitrogen). The fluorescence signals were captured with a confocal microscope (LSM800, Carl Zeiss Microscopy, Jena, Germany).

### CAFs conditioned-media collection

Conditioned-media (CM) was collected from nine CAFs, namely PC-B-004, PC-B-044, PC-B-053, PC-B-099, PC-B-120, PC-B-130, PC-B-132, PC-B-140, PC-B-142

and 2 NFs cultured in 10% FBS containing DMEM/F12 until 85–90% confluency before replacing it with 1% FBS containing DMEM/F12. CM was then centrifuged at 2000 g at 4°C for 5 min. The supernatant was stored at -80°C.

#### IL-6 measurement by enzyme-linked immunosorbent assay

The CM-derived IL-6 was detected by ELISA according to the instructions (R&D, MN). Absorbance values at 450 nm were determined with a plate reader (Epoch-Microplate-BioTek, CA). IL-6 concentration was determined by the line-curve fitting of standard results.

#### IL-6R knockdown by small interfering RNA

The  $2 \times 10^5$  cancer cells were cultured in a complete medium overnight. The transfection solution was prepared by mixing OptiMEM-I (Gibco) with either 160 pmol *siIL-6R* or Lipofectamine 3000 (Invitrogen), while a mock control was performed in the same manner without *siIL-6R*. The *siIL-6R* knockdown (KD) cells were stained with anti-IL-6R antibody (1:50, sc-373708; Santa Cruz, CA), followed by anti-mouse PE antibody (1:100, 22549814; ImmunoTools, Friesoythe, Germany) at 4°C for 1 h. The IL-6R level was checked by flow cytometry (Beckman Coulter Life Sciences, CA). Data were analyzed using FlowJo 10 software (Flowjo, LLC, OR).

#### Drug cytotoxicity using annexin V-APC/ PI staining

Cancer cells were treated with CM with or without 5  $\mu$ M Dox ( $IC_{50}$ ) (Sigma-Aldrich). After 48 h, cancer cells were stained by Annexin V-APC/propidium iodide (1:100, ImmunoTools) at 4°C for 1 h and then analyzed by flow cytometry (Beckman Coulter). The cell apoptosis was analyzed using FlowJo 10 software (Flowjo, LLC).

#### Western blot analysis

Cells were treated with various CM or 50 ng/ml recombinant human IL-6 (rhIL-6, 206-IL-050, R&D) for 48 h to detect PD-L1 and for 30 min to detect signaling pathway proteins. After lysing with RIPA buffer (Invitrogen, Thermo Fisher Scientific, MA) and quantitating protein by Bradford kits (Bio-Rad, CA), 40  $\mu$ g protein was loaded onto 10% SDS-PAGE and transferred to PVDF membrane (Bio-Rad). After blocking with 5% skim milk for 1 h, the membrane was incubated with the anti-human PD-L1 (1:500, ab205921; Abcam, Cambridge, UK) at 4°C overnight. The HRP-conjugated anti-rabbit (1:5000, ab6721; Abcam) or anti-mouse secondary antibodies (1:5000, ab6789; Abcam) were then incubated at RT for 1 h.

Cells were pre-treated with 2  $\mu$ M AKT inhibitor (21597; Chaman Chemical, MI) or 10  $\mu$ M Stattic (14590;

Chaman Chemical) for 2 h before treating with CM for 48 h. The anti-STAT3 (1:1000, 9139; Cell Signaling Technology, MA), anti-pSTAT3 (1:2000, ab76315; Cell Signaling), rabbit anti-AKT (1:1000, 9272, Cell Signaling), rabbit anti-pSTAT3 (1:1000, 9275; Cell Signaling), anti-ERK1/2 (1:1000, 9102; Cell Signaling), and anti-phosphoERK1/2 (1:1000, 9101; Cell Signaling) followed by HRP-conjugated anti-rabbit (1:5000, ab6721; Abcam) or anti-mouse (1:5000, ab6789; Abcam) were used. The ECL (Invitrogen) was visualized under Gel Document (SynGene, Cambridge, UK). The protein intensity was measured by ImageJ software version 1.48v. The  $\beta$ -actin was used to normalize the total loading protein using anti- $\beta$ -actin (1:20,000, sc-47778; Santa Cruz).

#### Production and characterization of FR $\alpha$ -CAR T cells

The production of FR $\alpha$ -CAR-T cells from healthy donor blood was previously described [25]. The lentiviral particles were quantified via titration in SupT1 cells [26]. Blood donors provided written consent under SIRB ethical approval (COA no. Si 225/2022). T cells were transduced by FR $\alpha$ -CAR lentiviruses at a multiplicity of infection (MOI) of 50 using 100  $\mu$ g/ml protamine sulfate (Sigma-Aldrich) and maintained in AIM-V (Gibco) with 5% human AB serum (Sigma-Aldrich), 20 ng/ml of IL-2 (ImmunoTools), 10 ng/ml of IL-7 (ImmunoTools) and 20 ng/ml of IL-15 (ImmunoTools) for 3 d.

T cells were phenotyped using eFluor<sup>TM</sup>450-anti-human CD3 (1:100, 48-0038-42; Invitrogen), APC-conjugated anti-human CD4 (1:100, 21270046; ImmunoTools), and PerCP-anti-human CD8 (1:100, 21810085; ImmunoTools). The FR $\alpha$ -CAR expression was determined by Pierce<sup>TM</sup> biotinylated protein-L (1:100, 29997; Invitrogen) and AlexaFluor<sup>®</sup>488-conjugated streptavidin (1:500, S32354; Invitrogen), then analyzed using flow cytometry (Beckman Coulter). Data were analyzed using FlowJo 10 software (Flowjo, LLC).

#### 2D and 3D culture cancer cell killing assays

For 2D culture, the mWasabi-luciferase-expressing target cancer cells (T) were treated with CM for 48 h. After removing the CM, the effector FR $\alpha$ -CAR effector T cells (E) were added at E:T ratios of 0.5:1, 1:1, and 2.5:1 for 24 h. Fluorescence images were taken under fluorescence microscopy (Olympus, Tokyo, Japan). The fluorescence intensity (FI) of target cells was detected (485/515 nm) using SynergyH1-Hybrid Reader (BioTek-Agilent, CA). The non-fluorescence-expressing cell lines were used as a blank control, while the target alone (control group) was used to normalize with all conditions regarded as no cytolysis (FI=1). The formula of relative FI = (FI of test-blank) / (FI of control-blank).

For 3D culture, the mWasabi-luciferase-expressing cells were seeded into an ultra-low attachment 96-well plate (CLS7007; Corning, MA) in 2.5% Matrigel® (354234, Corning). The spheroids were treated with CM on day 2 and cultured for 2 more days. Effector cells were labeled with CellTracker™ Orange CMRA (C34551; Invitrogen) before adding to target cells at E:T ratios of 2.5, 5:1, and 10:1, and then co-cultured for 4 d. Fluorescence images were detected by fluorescence microscopy (Olympus) and analyzed by CellSense Standard program version 1.15 (Olympus). The FI was analyzed by the ImageJ software 1.48v (<http://rsbweb.nih.gov/ij/>).

### Statistical analysis

Data were analyzed using one-way analysis of variance (ANOVA) or Student's *t* test. All statistical calculations were performed with GraphPad Prism software version 5 (GraphPad Software Inc., CA). The data are shown as mean ± SD and considered statistically significant when  $P < 0.05$ .

## Results

### Expression of fibroblast markers

CAFs showed the absence of CK epithelial markers, but the presence of VIM and ASMA mesenchymal markers [13]. FAP is used to classify aggressive CAF subtypes, while CD10/GPR77 markers are associated with drug resistance [27]. The results exhibited that all nine CAFs were negative for panCK and positive for both VIM and ASMA (Fig. 1). Among these nine CAFs, eight were FAP-positive CAFs (8/9 = 89%), PC-B-044, PC-B-053, PC-B-099, PC-B-120, PC-B-130, PC-B-132, PC-B-140, and PC-B-142, and one FAP-negative CAF (PC-B-004). All CAFs expressed GPR77 and eight CAFs except PC-B-004 expressed CD10. Notably, BNF showed negative FAP, CD10, and GPR77, while HDF was negative for FAP/CD10 and positive for GPR77.

### CAFs secreted high IL-6 levels and CAF-derived IL-6 induced PD-L1 expression in TNBC cells

Only IL-6 showed a significant increase in CAF-CM compared to CM from normal fibroblasts isolated from ovarian tissues (Additional file 1: Supplementary Method and Fig. S1). ELISA results confirmed that six of nine CAF-CM (67%) had significantly higher levels than BNF-CM

( $P < 0.05$ ), which was defined as the high IL-6 CM (PC-B-044, PC-B-053, PC-B-099, PC-B-120, PC-B-132, and PC-B-142) (Fig. 2A). In contrast, three CMs (PC-B-004, PC-B-130, and PC-B-140) were defined as the low IL-6 CM.

The IL-6R in *siIL-6R* KD MDA-MB-231 was 13% and 16% in *siIL-6R* KD HCC70 cells compared to those of scramble cells (69% in MDA-MB-231, 62% in HCC70 cells) (Fig. 2B). The levels of IL-6R in the scramble and parental cells were not different. No morphological and viable cell changes of *siIL-6R* KD cells were observed in both cells compared to those of parental and scramble cells.

The role of CAF-derived IL-6 in inducing PD-L1 expression was observed in MDA-MB-231 (Fig. 2C) and HCC70 cells (Fig. 2D). NF-CM treated scramble cells showed no significant differences in PD-L1 compared to that of untreated cells in both cells. The rhIL-6-treated scramble cells significantly induced PD-L1 compared to that of BNF-CM ( $P < 0.05$ ). Treating-scramble cells with high IL-6 CM (PC-B-044, PC-B-120, PC-B-132, and PC-B-142) significantly induced PD-L1 in both BCA cells compared to those of BNF-CM ( $P < 0.05$ ). Interestingly, *siIL-6R* KD cells showed no response to high IL-6-CM-induced PD-L1 expression in both cell lines.

### The CAF-derived IL-6 induced Dox resistance

Dox significantly induced apoptosis of scramble MDA-MB-231 cells compared to untreated cells ( $P < 0.01$ ) (Fig. 3A). Low IL-6 PC-B-004-CM and BNF-CM pretreated cells showed the same level of apoptotic cells to no CM-pretreated cells. Interestingly, high IL-6 CMs stimulated Dox-induced apoptosis ( $28.0 \pm 5.7\%$  for PC-B-044 CM,  $33.0 \pm 2.0\%$  for PC-B-120 CM,  $33.3 \pm 3.1\%$  for PC-B-132 CM, and  $21.5 \pm 9.2\%$  for PC-B-142 CM,  $P < 0.05$ ), but this was significantly lower cell apoptosis than that of low IL-6 CM treatment. This implies that high IL-6 CM reduced cell sensitivity to Dox-induced apoptosis. In IL-6R KD cells, the sensitivity to Dox could significantly restore to the same level of Dox-treated scramble cells ( $P < 0.01$ ) and significantly increased compared to the apoptotic cells of high IL-6-CM-treated intact IL-6R cells ( $P < 0.05$ ). Similar results of high IL-6-CM reduced Dox-induced apoptosis of HCC70 cells and the restoration of drug sensitivity in the impaired

(See figure on next page.)

**Fig. 1** Characterization of primary culture fibroblasts. Immunofluorescence using antibodies directed to specific markers for epithelial cells (panCK, red fluorescence), fibroblast intermediate filament (VIM, red fluorescence), myofibroblasts (ASMA, red fluorescence), fibroblast-associated protein (FAP, green fluorescence), and chemotactic receptor (CD10, green fluorescence; GPR77, red fluorescence) of different primary culture fibroblasts and normal fibroblasts (HDF and BNF). The nuclei were counterstained with Hoechst. All images were captured at 200× magnification, scale bars = 50 μm. NFs, normal fibroblasts; HDF, human dermal fibroblast; BNF, breast normal fibroblast; CAFs, cancer-associated fibroblasts; panCK, pan-cytokeratin; VIM, vimentin; ASMA, alpha-smooth muscle actin; FAP, fibroblast activation protein; CD10, a cluster of differentiation 10; GPR77, G protein-coupled receptor 77



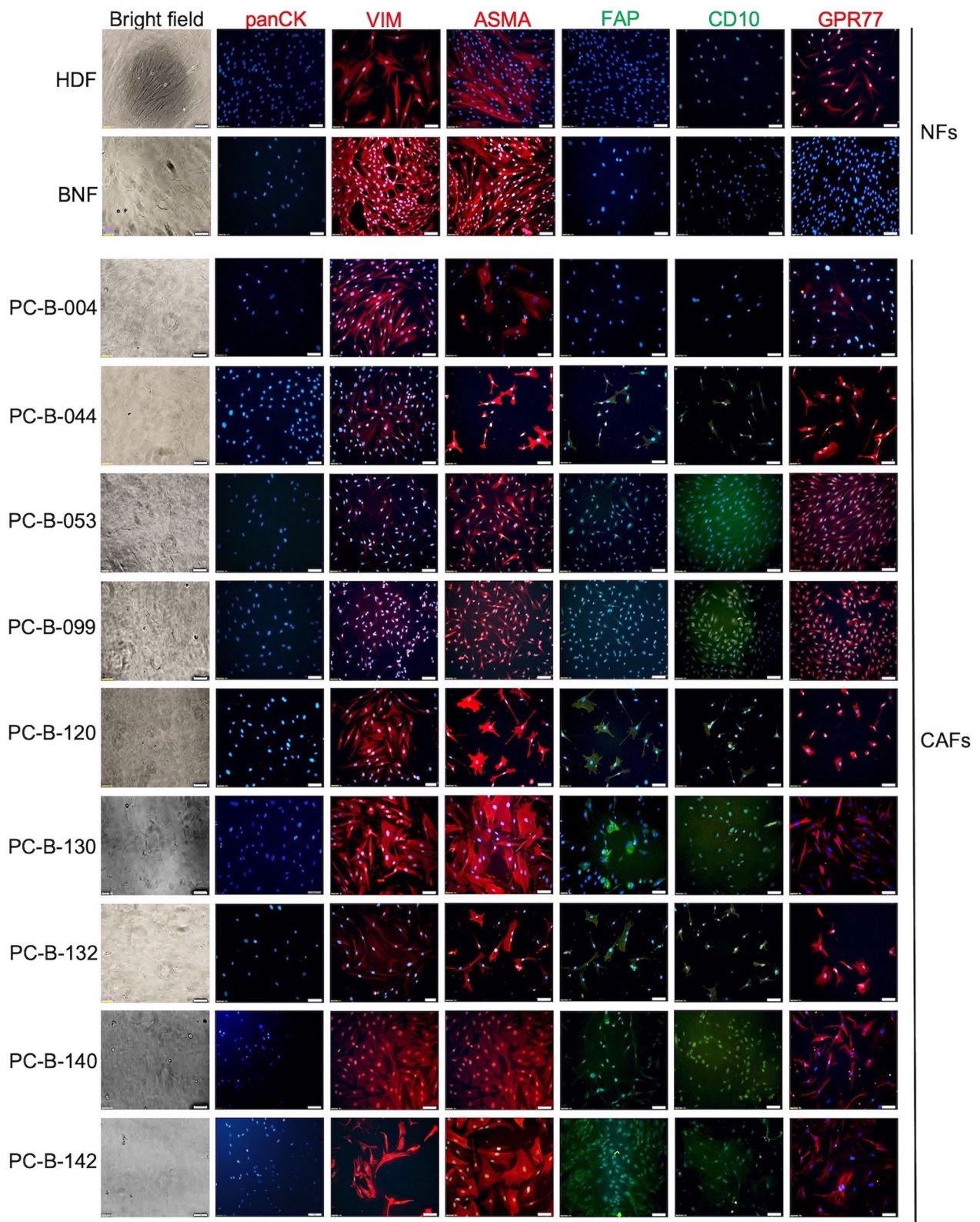


**Fig. 1** (See legend on previous page.)

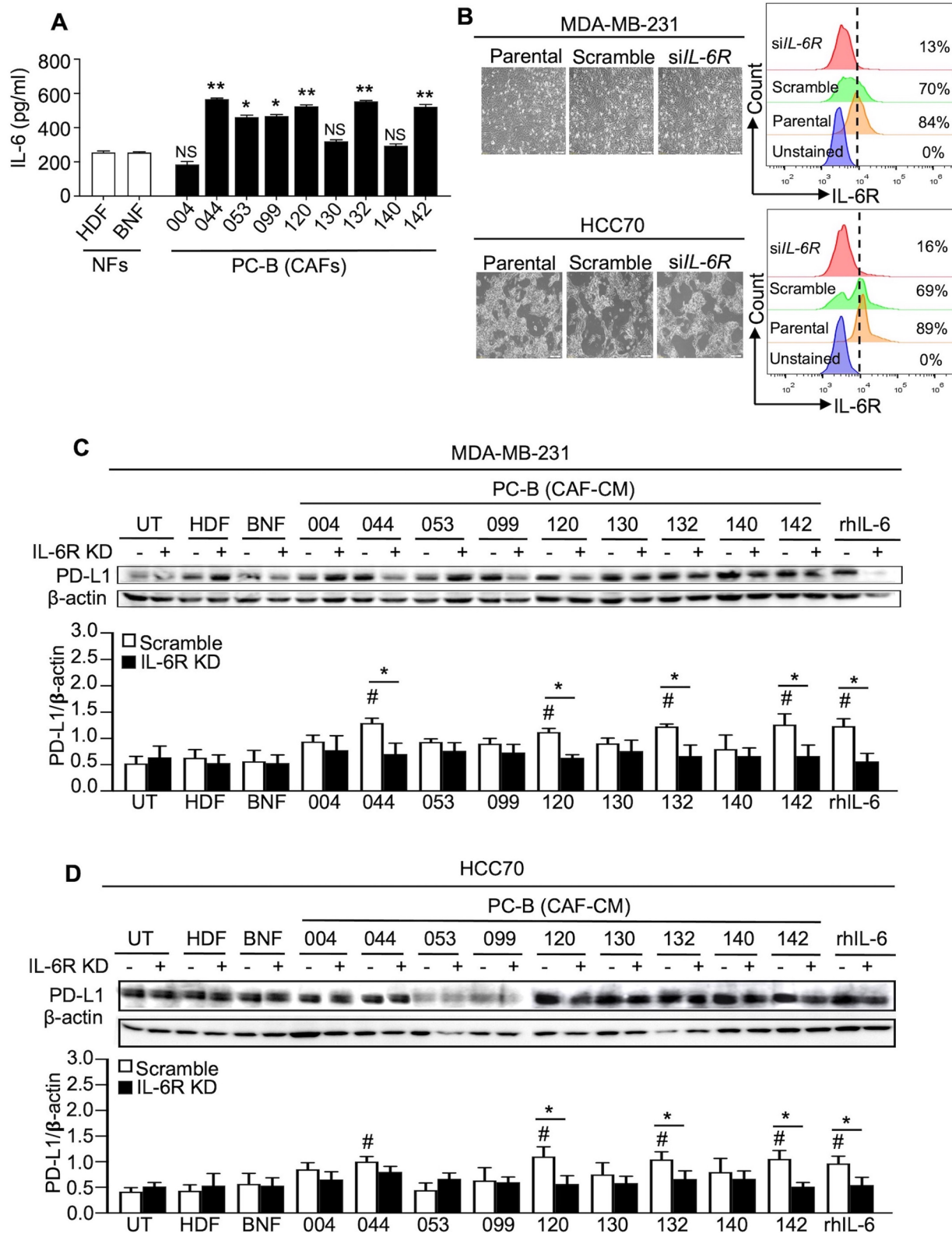


**Fig. 2** (See legend on next page.)

(See figure on previous page.)

**Fig. 2** CAF-derived IL-6 and its effect on PD-L1 expression. **A** The level of IL-6 in CMs of different NFs and CAFs. Bar graphs represent the mean  $\pm$  SD of three independent experiments. \* $P < 0.05$ , \*\* $P < 0.01$  compared to BNF using one-way ANOVA. NS, no significance. **B** The representative morphology of parental MDA-MB-231 and HCC70 cells, scramble, and *siIL-6R* KD cells and the representative histogram of IL-6R detection by flow cytometry. **C, D** Effect of CAF-derived IL-6 on PD-L1 in MDA-MB-231 and HCC70 scramble and *siIL-6R* KD cells determined by Western blot analysis.  $\beta$ -actin was used as a housekeeping reference protein for semiquantitative analysis. Bar graphs represent the mean  $\pm$  SD of three independent experiments. # $P < 0.05$  compared to UT condition using one-way ANOVA. \* $P < 0.05$  compared within group using Student's *t* test. CMs, conditioned-media; NFs, normal fibroblasts; HDF, human dermal fibroblasts; BNF, breast normal fibroblast; CAFs, cancer-associated fibroblasts; NS, no significance; IL-6R KD, IL-6R knocked down; UT, untreated cells; rhIL-6, recombinant human IL-6

IL-6R HCC70 cells were observed (Fig. 3B). These findings indicate that CAF-derived IL-6 increases Dox resistance partly through IL-6/IL-6R interaction.

#### CAF-derived IL-6 induced PD-L1 expression via STAT3 and AKT signaling pathways

For MDA-MB-231, pSTAT3 was significantly induced by all high IL-6 CM (PC-B-044, PC-B-120, PC-B-132, and PC-B-142), while pAKT was activated by only PC-B-132 and PC-B-142 ( $P < 0.05$ ) (Fig. 4A). In the CM-treated IL-6R KD cells, pSTAT3, pAKT, and pERK had no significant upregulation compared to those of scramble MDA-MB-231 and HCC70 cells. This induction was attenuated when cells had impaired IL-6R expression. The same pattern of results was observed in HCC70 cells (Fig. 4B). In addition to pSTAT3 and pAKT, rhIL-6-treated cells could induce pERK in both cells (Fig. 4A, B). The results suggest that high IL-6-CM activated pSTAT3 and pAKT signaling pathways, but no changes of pERK, probably via IL-6R.

Without Stat3 or AKT inhibitors, PD-L1 in cells treated with low IL-6 CM (PC-B-004) showed no significant differences compared to that of BNF-CM treatment, whereas high IL-6 CM (PC-B-132 and PC-B-142) significantly induced PD-L1 ( $P < 0.05$ ) in MDA-MB-231 (Fig. 4C) and HCC70 (Fig. 4D). Blocking with Stat3 or AKT inhibitors significantly decreased the PD-L1 levels of high IL-6-CM treatment compared to without inhibitors in both cells.

#### CAF-derived IL-6 compromised FR $\alpha$ -CAR T cell killing ability

The cancer cell killing ability of FR $\alpha$ -CAR T cells in 2D (Fig. 5) and 3D cancer cell culture (Fig. 6) was observed.

In the 2D killing assay, coculturing of FR $\alpha$ -CAR-T cells (E) with FR $\alpha$  expressing-target cancer cells (T), MDA-MB-231 and HCC70 cells (Additional file 2: Fig. S2) at E:T of 0.5:1, 1:1, and 2.5:1 reduced fluorescence intensity of viable target cells, with a significant reduction level at only 2.5:1 ( $P < 0.01$ ) (Fig. 5A, B). A similar capability of FR $\alpha$ -CAR-T cells was observed in low IL-6 CM (BNF, PC-B-004)-treated cells in both MDA-MB-231 and HCC70 cells ( $P < 0.05$ ) (Fig. 5A, B). In contrast, both MDA-MB-231 and HCC70 cells exposed to high IL-6 CM (PC-B-132 and -142) showed resistance to FR $\alpha$ -CAR-T cell killing activity. Similar results were exhibited in the 3D killing assay in the same manner (Fig. 6A, B). Interestingly, in 3D culture system, FR $\alpha$ -CAR T cells and cancer cells coculture reduced the viability of cancer cells in a dose-dependent manner with statistical significance.

#### Discussion

CAFs produce many substances such as IL-6, IL-8, and TGF- $\beta$  impacting cancer progression and immunosuppression [6–9, 14]. TGF- $\beta$  activated CAFs to secrete IL-6 resulting in the enhancement of CRC metastasis [28]. IL-6 is a major factor of BCA-CAF secretion that can induce resistance to anti-estrogens [29]. In HCC, CAFs were the major source of IL-6 [30]. High IL-6 expression CAFs greatly decreased CD8<sup>+</sup> T cell infiltration in tumors [30]. CAFs-derived IL-6 induced pancreatic cancer cell migration and invasion [31]. CAF-secreted IL-6 reduced NK cells' function in CRC cells by promoting monocyte differentiation into M2 macrophages and recruiting to the tumor [32, 33]. No investigation, however, has assessed the role of CAF-derived IL-6 in T cell function regulation via induction of PD-L1 in BCA. In this current study, CAF-derived IL-6 exhibited a significantly higher

(See figure on next page.)

**Fig. 3** Effect of CAF-derived IL-6 on Dox-induced apoptosis. BCA cell lines after incubation in the presence of CM with or without Dox (5  $\mu$ M) for 48 h. **A** The apoptosis of MDA-MB-231 and **B** HCC70 after staining with the Annexin V-APC/PI and analyzing by flow cytometry. The representative dot plots of cell apoptosis and the percentage of cell apoptosis in the bar graph (means  $\pm$  SD of three independent experiments) are shown. # $P < 0.05$ , ## $P < 0.01$  compared to CM-free and Dox-free condition using one-way ANOVA, \$\$\$ $P < 0.001$ , \$\$\$\$ $P < 0.0001$  compared to CM-free with Dox condition using one-way ANOVA, \* $P < 0.05$  compared within the group using Student's *t* test. FSC-A, forward scatter area; SSC-A, side scatter area; UT, untreated cells; Dox, doxorubicin; BNF, breast normal fibroblast; CM, conditioned medium; IL-6R KD, IL-6R knocked down; rhIL-6, recombinant human IL-6



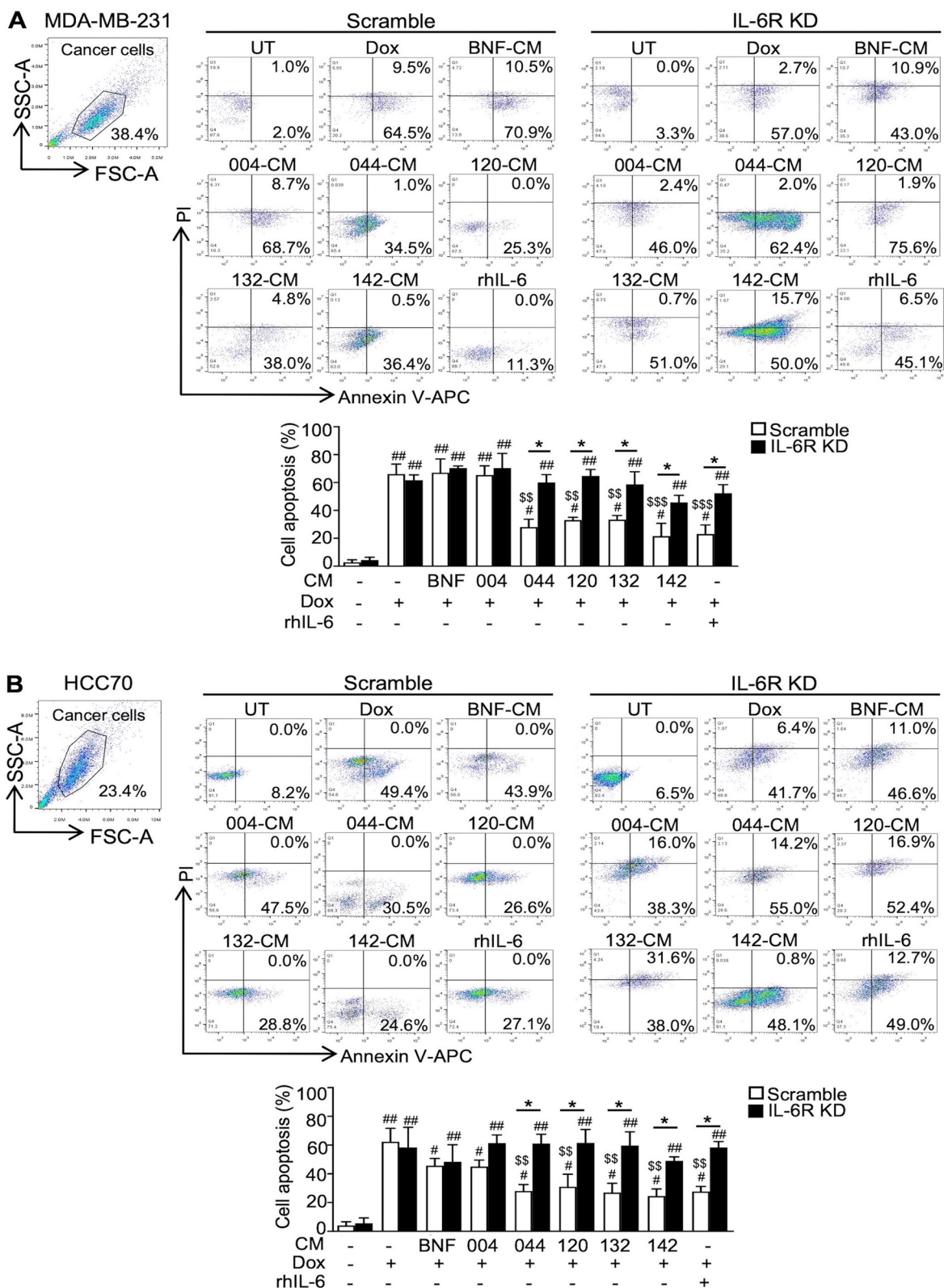


**Fig. 3** (See legend on previous page.)



level among other cytokines. IL-6 releases into TME and may be involved in cancer progression, immunosuppression, and the responses of cancer cells to chemotherapy and immunotherapy.

CAFs were positive for vimentin (VIM) and alpha-smooth muscle actin (ASMA), but negative for cytokeratin (CK) expression ensuring that CAFs culture is not contaminated by cancer cells [13]. The immunosuppressive role of FAP<sup>+</sup> CAFs has been extremely studied in various types of cancers such as head and neck, pancreatic, breast, lung, and liver cancers [13]. In head and neck cancer, FAP<sup>+</sup> CAFs inhibited CD8<sup>+</sup> T cell proliferation and promoted regulatory T cell (Treg) recruitment by secreting TGF- $\beta$  and IL-6 [34]. In the BCA mouse model, the elimination of FAP<sup>+</sup> CAFs showed an increasing CD8<sup>+</sup> T cell population [35]. IL-6 from CD10<sup>+</sup> GPR77<sup>+</sup> CAFs promoted tumor formation in lung cancer [27, 36]. CD10<sup>+</sup> GPR77<sup>+</sup> CAFs enriched a survival niche for cancer stem cells (CSCs), enhanced tumor formation, and induced cancer chemoresistance by secreting IL-6 leading to driving the activation of NF- $\kappa$ B via p65 phosphorylation and acetylation, which maintained by complement signaling via GPR77 [27]. Targeting the CD10<sup>+</sup> GPR77<sup>+</sup> CAFs subset retards tumor formation and reverses chemoresistance by destroying the CSC niches [27, 36]. CD10<sup>+</sup> GPR77<sup>+</sup> FAP<sup>+</sup> CAFs were associated with chemoresistance and overall survival of advanced gastric cancer patients who underwent neoadjuvant chemotherapy (NCT) [37]. FAP increasing drug resistance are various, such as promoting immunosuppression and producing chemokine [37]. CD10 and GPR77 have been proven to promote cancer formation and chemoresistance by providing a survival niche for CSCs and promoting an epithelial-mesenchymal transition [37]. In addition, CAFs affect the chemotherapy through an increased interstitial fluid pressure forming a barrier to the transcapillary transport of drugs from blood vessels to cancer cells [38]. All mentioned evidence supports the present results that high IL-6-secreting CAFs were positive for CD10<sup>+</sup> GPR77<sup>+</sup> FAP<sup>+</sup> which may correlate with drug resistance and may regulate anti-tumor immune responses.

In addition to the IL-6 derived from CAFs, IL-6 can be secreted from BCA cells which then promotes cancer cell metastasis in an autocrine effect [39, 40]. Cancer cell-derived IL-6 acted to promote tumorigenesis in BCA, HCC, and lung cancer [41, 42]. Secreted IL-6 binding to membrane IL-6R induces STAT3 expression which is aberrantly active in BCA to promote cancer proliferation and anti-apoptosis [43, 44]. Moreover, STAT3 cooperates with NF- $\kappa$ B in IL-6 induction and the IL-6/STAT3 pathways synergize in the induction of c-MYC leading to promoting cancer cell survival [45].

In contrast to the tumor-promoting effect of IL-6 through the classical IL-6 signaling via membrane IL-6R and glycoprotein 130 (gp130) subunit, in some cancers, IL-6 trans-signaling which is a complex of IL-6 and the soluble IL-6R and membrane gp130 [46], but not IL-6 classic signaling, is mandatory for the development of liver carcinogenesis [46]. Therefore, specific inhibition of IL-6 trans-signaling, rather than total inhibition of IL-6 signaling, is sufficient to blunt tumor initiation and impair tumor progression without compromising IL-6 classic signaling-driven protective immune responses.

CAFs contribute to chemoresistance and immunotherapeutic resistance by upregulating immune checkpoint molecules [22, 23]. The CAF-derived IL-6 promoted PD-L1 expression via STAT3 and AKT pathways and specific inhibitors against pSTAT3 and pAKT attenuated PD-L1 expression induction by IL-6-derived CAF-CM. HCC-CAFs-induced PD-L1<sup>+</sup> neutrophils through the IL6-STAT3 pathway involved in immunosuppression were previously reported [22]. Moreover, the activation of the STAT3-PI3K/AKT pathway leads to high expression of PD-L1 in various types of cancers [47]. PD-L1 expression is transcriptionally regulated by STAT3 and MYC [48]. The pSTAT3 dimers directly bind on the PD-L1 gene promoter inducing its expression [49] which has been detected in non-small cell lung cancer [50] and head and neck squamous cell carcinoma [51]. The immunosuppressive PD-1/PD-L1 pathway participates in cancer immune escape via the abnormal activation of the tumor-intrinsic STAT3-PI3K/AKT pathway leading to high expression of PD-L1 resulting in attenuation of anti-tumor T cell responses. Interestingly, IL-6 pathway

(See figure on next page.)

**Fig. 4** Effect of CAF-derived IL-6 on PD-L1 expression through STAT3 and AKT pathways and the blockage with specific inhibitors. **A** Scramble and *siIL-6R* KD cells after pre-treating with CM for 30 h to observe the phospho- and total protein levels of STAT3, AKT, and ERK using Western blot analysis in MDA-MD231 and **B** HCC70 cell lines. The levels of phosphoproteins were normalized against relative total protein and  $\beta$ -actin. **C** The level of PD-L1 of MDA-MD231 and **D** HCC70 following blocking with STAT3 (Stattic) or AKT (AT) inhibitors for 2 h.  $\beta$ -actin was used for semiquantitative analysis. Bar graphs represented as mean  $\pm$  SD of 3 independent experiments. <sup>#</sup> $P < 0.05$ , <sup>##</sup> $P < 0.01$  compared to BNF using one-way ANOVA, <sup>\*</sup> $P < 0.05$  compared within group using Student's *t* test. UT, untreated cells; BNF, breast normal fibroblast; CAFs, cancer-associated fibroblasts; CM, conditioned-medium; IL-6R KD, IL-6R knocked down; rhIL-6, recombinant human IL-6

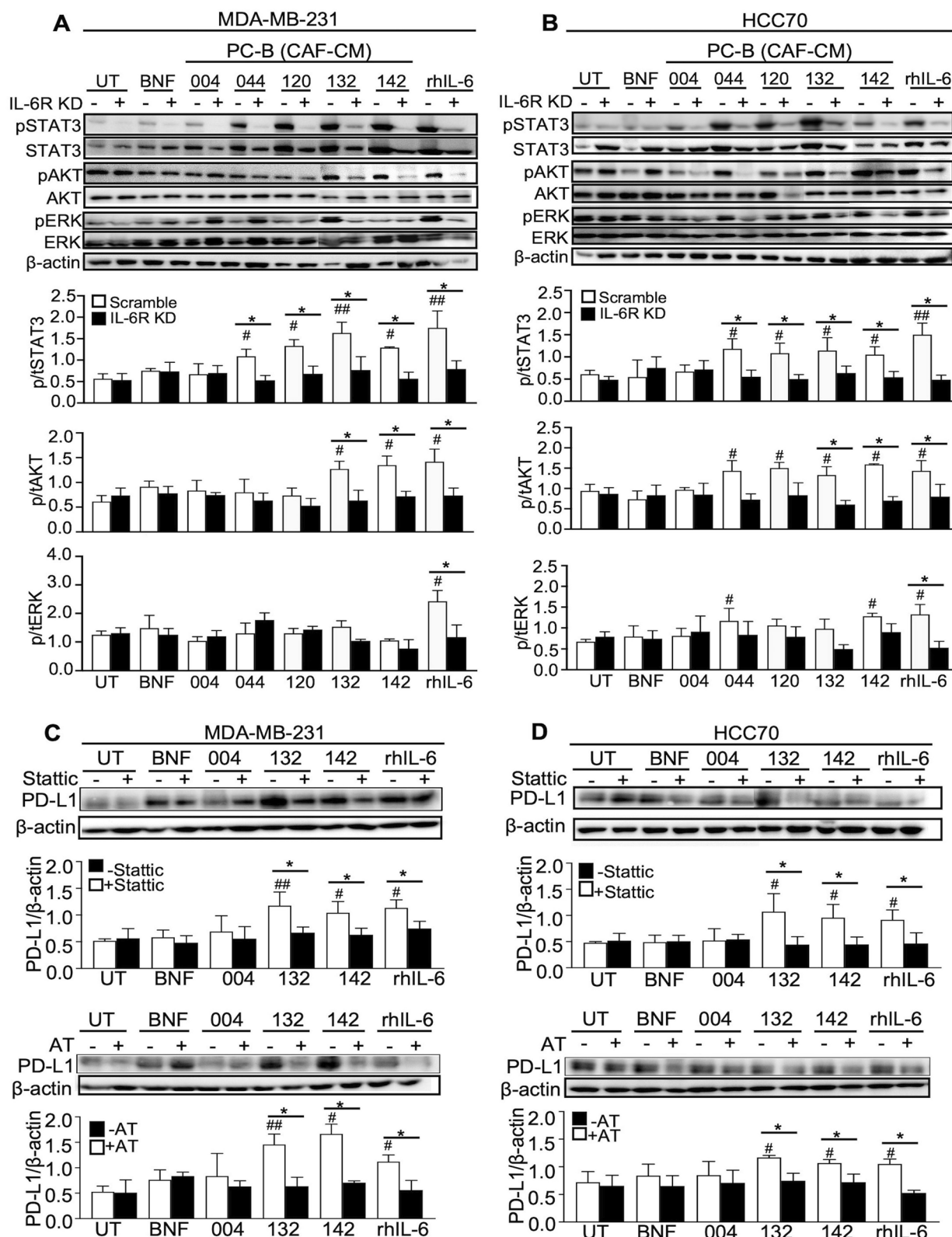
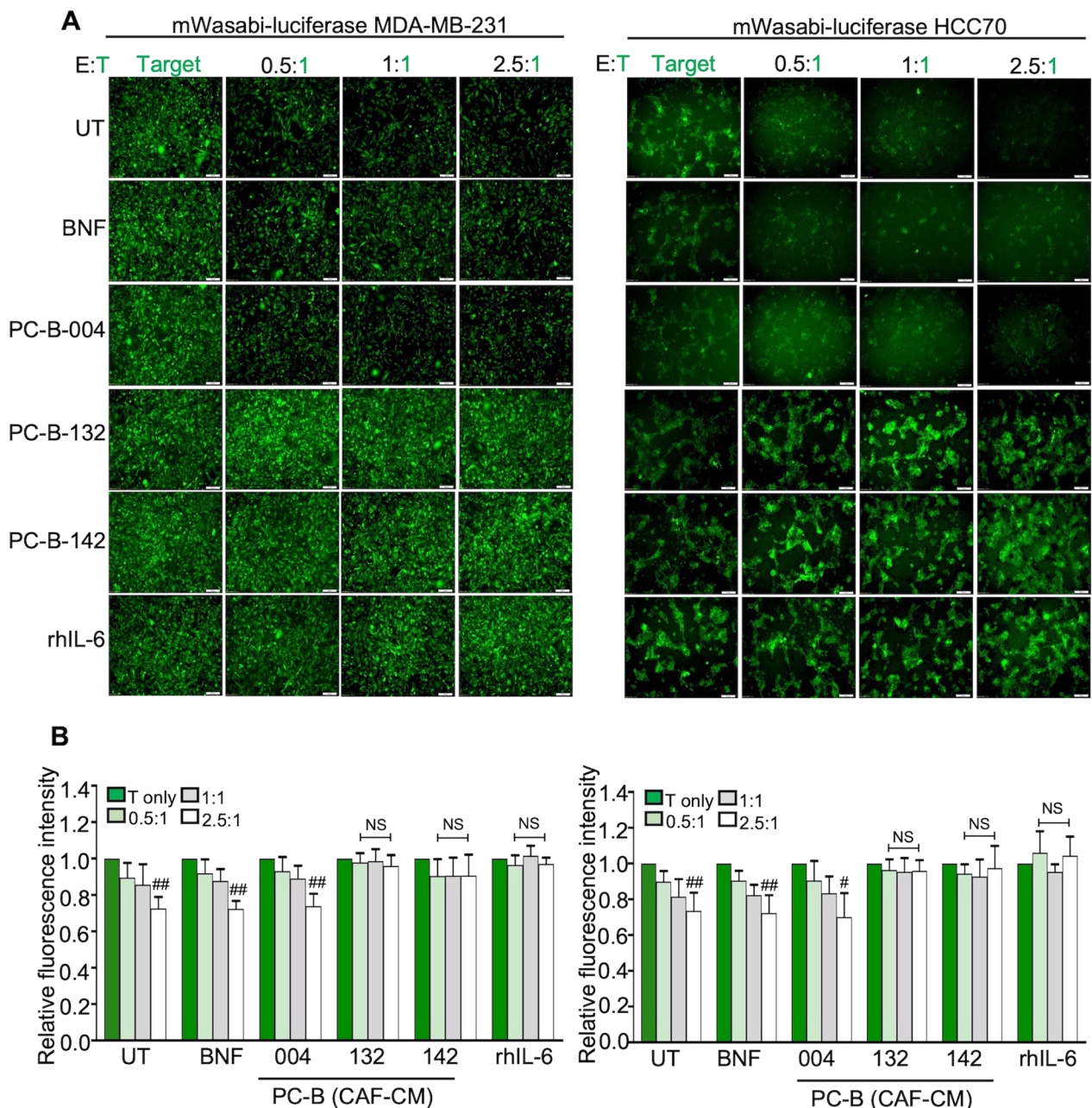


Fig. 4 (See legend on previous page.)



**Fig. 5** CAF-derived IL-6 compromised FR $\alpha$ -CAR-T cell killing ability in 2D cancer cell culture. **A** The representative of fluorescence images shows mWasabi-luciferase expressing target cells (T) after pre-treating with CM and coculturing with effector FR $\alpha$ -CAR-T cells (E) at E:T ratios of 0.5:1, 1:1, and 2.5:1 for 24 h (scale bars = 100  $\mu$ m). The target-only condition (T-only) indicates target cancer cells without coculturing with effector T cells. **B** Bar graphs showing the killing ability of FR $\alpha$ -CAR-T cells from 2 donors (mean  $\pm$  SD of three independent experiments of each donor). \* $P$  < 0.05, \*\* $P$  < 0.01 compared to the T-only condition using one-way ANOVA. UT, untreated cells; BNF, breast normal fibroblast; CAFs, cancer-associated fibroblasts; CM, conditioned-medium; IL-6R KD, IL-6R knocked down; rhIL-6, recombinant human IL-6; NS, no significance

inhibitors are currently tested in combination with chemotherapy in patients with BCA (NCT03135171), pancreatic cancer (NCT04258150, NCT02767557), or liver cancer (NCT04338685), who displayed potent anti-cancer activity with a low incidence of IL-6 drug toxicity [6].

The PD-L1 expression decreased by hesperidin through inhibition of AKT and NF- $\kappa$ B signaling pathways in the MDA-MB-231 cell line [19]. These reports confirm present findings that IL-6 can inhibit antitumor immunity

by promoting PD-L1 expression via STAT3 and AKT pathways.

It is suggested that targeting the IL-6/IL-6R/STAT3 axis is expected to become an important strategy for BCA treatment [52]. IL-6 acts directly on cancer cells to induce the expression of STAT3-encoding proteins driving cancer proliferation, i.e., cyclin D1 and survival, i.e., BCL2-like protein 1 (BCL-xL). Early-phase trials exploring the safety and effectiveness of tocilizumab (anti-IL-6RmAb) in BCA patients are currently ongoing (NCT03135171) [52]. Some high IL-6-containing-CMs, however, did not alter PD-L1 expression. These may be explained by the possibility that CAF secreted various substances which may affect IL-6 secretion by CAFs such as CXCL10 [6, 31]. Current evidence points to chemotherapy-induced DNA damage with nanoparticle albumin bound-paclitaxel (Nab-PTX) influencing the repertoire of CAF-secreted factors after treatment [31]. Nab-PTX treatment increases CXCL-10 expression in pancreatic cancer cells leading to reduced secretion of CAF-derived IL-6 subsequently impairing cancer migration and invasion [31].

DNA damage during chemotherapy is sensed by cyclic GMP-AMP synthase, a stimulator of interferon genes (STING). Dox-mediated DNA damage induced STING-mediated NF- $\kappa$ B activation in TNBC cell lines resulting in the induction of IL-6 secretion which could activate pSTAT3 leading to cancer cell survival enhancement and an immune-suppressive mechanism by PD-L1 expression induction [53]. The cancer cells containing DNA double-strand breaks increased IL-6 secretion by DNA damage response proteins such as ataxia-telangiectasia-mutated during oncogene-induced senescence [54]. Moreover, IL-6 could induce ATM kinase leading to DNA damage repair [55].

Moreover, CAFs reprogramming by vitamin A and vitamin D were shown to inhibit tumor-supportive secretomes [6, 56]. Vitamin A and vitamin D reprogramming strategies are both associated with TGF- $\beta$  signaling pathway inhibition. Indeed, vitamin D decreases fibroblast activation [57], whereas vitamin A inhibits

the fibroblasts' capacity to release active TGF- $\beta$ , thus impeding CAF-secreted factors that are associated with the chemo- and immunotherapeutic resistance [58]. Additional research with a better understanding of the mechanisms of CAF secreted-substances that affect IL-6 secretion is needed to confirm.

Importantly, the previous studies of IL-6 in animal models support our findings that IL-6 mediated drug resistance and induced PD-L1 expression. Activation of IL-6 inflammatory loop-induced trastuzumab resistance in breast cancer mouse xenografts [59]. Using a Bcl-2 antagonist (sabutoclax) could inhibit the IL-6/STAT3 signaling to resensitize Dox-resistant breast cancer in vitro and in vivo models [60]. Blocking of STAT3 can prolong the survival time of tumor-bearing mice by suppressing tumor growth and increasing Dox sensitivity in osteosarcoma [61]. Moreover, the combination of IL-6 blockades and anti-PD-L1 antibodies reduced cancer progression in mouse pancreatic cancer [62].

CAR-T cell immunotherapy has emerged as a cancer therapeutic strategy [63]. FR $\alpha$  expression is associated with poor prognosis in BCA patients [64]. Several FR $\alpha$ -targeting immunotherapies, such as monoclonal antibody [65] and adoptive T cell therapy [66], have been developed. In the present study, FR $\alpha$  expression was found in TNBC cell lines which is consistent with a prior study that reported the high prevalence of FR $\alpha$  in TNBC [67]. It was proven that FR $\alpha$ -CAR-T cells specifically lysed FR $\alpha$ -expressing cells in vitro [25]. These current findings indicate that CAF-derived IL-6 increases PD-L1-attenuated CAR-T cell cytotoxicity (Fig. 6C). Targeting CAF-derived cytokines and chemokines in combination with immunotherapies can improve anticancer efficiency such as when targeting the CXCL12-CXCR4 axis reverses FAP+CAF-mediated immunosuppression and synergizes with anti-PD-L1 immunotherapy in pancreatic cancer [68]. In conclusion, therapeutics aim at interfering with the IL6/IL-6R and PD-1/PD-L1 pathways may be combined to improve the response to chemotherapy and cell therapy in TNBC patients.

(See figure on next page.)

**Fig. 6** CAF-derived IL-6 attenuated FR $\alpha$ -CAR T cell cytotoxicity in 3D cancer cell culture. **A** The representative of spheroids of mWasabi-luciferase expressing target cells (T) after pre-treating with CM and coculturing with effector FR $\alpha$ -CAR T cells (E) at E:T ratios of 2.5:1, 5:1, and 10:1 for 4 days (scale bars = 100  $\mu$ m). The target-only condition (T-only) indicates target cells without effector cells. **B** Bar graphs show the killing ability of FR $\alpha$ -CAR-T cells from two donors (means  $\pm$  SD of three independent experiments of each donor). \* $P$  < 0.05, \*\* $P$  < 0.01, \*\*\* $P$  < 0.001 compared to the T-only condition using one-way ANOVA. **C** The proposed mechanism of CAF-derived IL-6 in promoting resistance to chemo- and immunotherapy. CAFs secrete high IL-6 which can bind to IL-6R on BCA cells. CAF-derived IL-6 induces Dox resistance by promoting cancer cell survival and promoting PD-L1 production through STAT3 and AKT signaling pathways. This PD-L1 induction by CAF-derived IL-6 can be attenuated by STAT3 and AKT inhibitors. The high PD-L1 expressing cancer cells suppress FR $\alpha$ -CAR-T cell killing ability. UT, untreated cells; BNF, breast normal fibroblast; CAFs, cancer-associated fibroblasts; CM, conditioned medium; IL-6R KD, IL-6R knocked down; rhIL-6, recombinant human IL-6; NS, no significance. BCA; breast cancer, FR $\alpha$ ; folate receptor alpha, PD-L1; programmed death ligand 1, PD-1; programmed death 1, CART cell; chimeric antigen receptor T cell



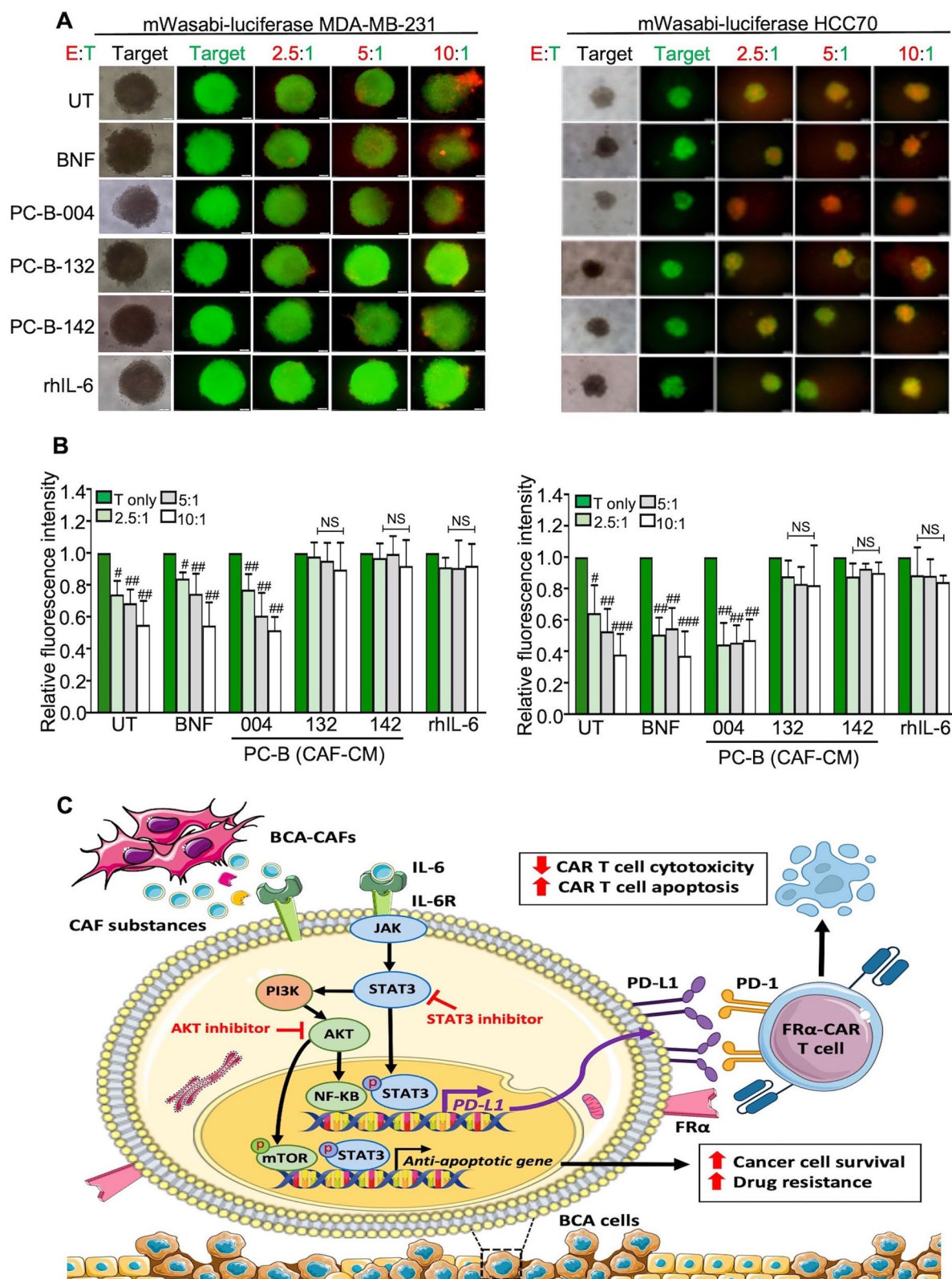


Fig. 6 (See legend on previous page.)

## Supplementary Information

The online version contains supplementary material available at <https://doi.org/10.1186/s13058-023-01684-7>.

**Additional file 1. Supplement Fig. 1.** CAF-derived substances in different primary culture fibroblasts.

**Additional file 2. Supplement Fig. 2.** Surface FR $\alpha$  expression on cell lines and transduction efficiency of FR $\alpha$  CAR-induced T cells from human primary T lymphocytes.

### Acknowledgements

The authors would like to thank Prof. James A. Will, USA, for the English edition.

### Author contributions

All authors contributed to the study's conception and design. Material preparation and data collection and analysis were performed by NC, PJ, SY, and PL. ST, MJ, PT, and PY contributed to data analysis and discussion. The first draft of the manuscript was written by NS and finalized by CT. All authors read and approved the final manuscript.

### Funding

This work was supported by Mid-Research Grant (N42A650343) funded by National Research Council of Thailand and Mahidol University to CT, and Siriraj Research Fund, Faculty of Medicine Siriraj Hospital, Mahidol University (Grant Number: R016532012 to NC).

### Availability of data and materials

The datasets used and/or analyzed during the current study are available from the corresponding author on reasonable request.

### Declarations

#### Ethics approval and consent to participate

All the experiments were performed according to the guidelines issued by the Ethics Committee of Siriraj Institutional Review Board, Faculty of Medicine Siriraj Hospital, Mahidol University. All participants signed written informed consent.

#### Consent for publication

All authors have read and approved the final version of the manuscript for publication.

#### Competing interests

The authors have no relevant financial or non-financial interests to disclose.

#### Author details

<sup>1</sup>Department of Immunology, Faculty of Medicine Siriraj Hospital, Mahidol University, Bangkok 10700, Thailand. <sup>2</sup>Siriraj Center of Research Excellence for Cancer Immunotherapy, Research Department, Faculty of Medicine Siriraj Hospital, Mahidol University, Bangkok 10700, Thailand. <sup>3</sup>Division of Molecular Medicine, Research Department, Faculty of Medicine Siriraj Hospital, Mahidol University, Bangkok 10700, Thailand.

Received: 5 February 2023 Accepted: 7 July 2023

Published online: 21 July 2023

### References

- Huang J, Chan PS, Lok V, Chen X, Ding H, Jin Y, Yuan J, Lao XQ, Zheng ZJ, Wong MC. Global incidence and mortality of breast cancer: a trend analysis. *Aging* (Albany NY). 2021;13(4):5748–803.
- Sung H, Ferlay J, Siegel RL, Laversanne M, Soerjomataram I, Jemal A, Bray F. Global cancer statistics 2020: GLOBOCAN estimates of incidence and mortality worldwide for 36 cancers in 185 countries. *CA Cancer J Clin*. 2021;71(3):209–49.
- Waks AG, Winer EP. Breast cancer treatment: a review. *JAMA*. 2019;321(3):288–300.
- Gupta GK, Collier AL, Lee D, Hoefler RA, Zheleva V, Siewertsz van Reesema LL, Tang-Tan AM, Guye ML, Chang DZ, Winston JS, et al. Perspectives on triple-negative breast cancer: current treatment strategies, unmet needs, and potential targets for future therapies. *Cancers* (Basel). 2020;12(9):2392.
- Turley SJ, Cremasco V, Astarita JL. Immunological hallmarks of stromal cells in the tumour microenvironment. *Nat Rev Immunol*. 2015;15(11):669–82.
- Linares J, Marin-Jimenez JA, Badia-Ramentol J, Calon A. Determinants and functions of CAFs secretome during cancer progression and therapy. *Front Cell Dev Biol*. 2020;8: 621070.
- Matsuo Y, Ochi N, Sawai H, Yasuda A, Takahashi H, Funahashi H, Takeyama H, Tong Z, Guha S. CXCL8/IL-8 and CXCL12/SDF-1 $\alpha$  co-operatively promote invasiveness and angiogenesis in pancreatic cancer. *Int J Cancer*. 2009;124(4):853–61.
- Wang X, Sun X, Mu L, Chen W. Cancer-associated fibroblasts induce epithelial-mesenchymal transition in endometrial cancer cells by regulating pituitary tumor transforming gene. *Cancer Invest*. 2019;37(3):134–43.
- Arwert EN, Milford EL, Rullan A, Derzsi S, Hooper S, Kato T, Mansfield D, Melcher A, Harrington KJ, Sahai E. STING and IRF3 in stromal fibroblasts enable sensing of genomic stress in cancer cells to undermine oncolytic viral therapy. *Nat Cell Biol*. 2020;22(7):758–66.
- Ding X, Ji J, Jiang J, Cai Q, Wang C, Shi M, Yu Y, Zhu Z, Zhang J. HGF-mediated crosstalk between cancer-associated fibroblasts and MET-unamplified gastric cancer cells activates coordinated tumorigenesis and metastasis. *Cell Death Dis*. 2018;9(9):867.
- Wu X, Tao P, Zhou Q, Li J, Yu Z, Wang X, Li J, Li C, Yan M, Zhu Z, et al. IL-6 secreted by cancer-associated fibroblasts promotes epithelial-mesenchymal transition and metastasis of gastric cancer via JAK2/STAT3 signaling pathway. *Oncotarget*. 2017;8(13):20741–50.
- Ziani L, Chouaib S, Thiery J. Alteration of the antitumor immune response by cancer-associated fibroblasts. *Front Immunol*. 2018;9:414.
- Liu T, Han C, Wang S, Fang P, Ma Z, Xu L, Yin R. Cancer-associated fibroblasts: an emerging target of anti-cancer immunotherapy. *J Hematol Oncol*. 2019;12(1):86.
- Costa A, Kieffer Y, Scholer-Dahirel A, Pelon F, Bourachot B, Cardon M, Sirven P, Magagna I, Fuhrmann L, Bernard C, et al. Fibroblast heterogeneity and immunosuppressive environment in human breast cancer. *Cancer Cell*. 2018;33(3):463–79.
- Masjedi A, Hashemi V, Hojjat-Farsangi M, Ghalamfarsa G, Azizi G, Yousefi M, Jadidi-Niaragh F. The significant role of interleukin-6 and its signaling pathway in the immunopathogenesis and treatment of breast cancer. *Biomed Pharmacother*. 2018;108:1415–24.
- Nakajima T, Kinoshita S, Sasagawa T, Sasaki K, Naruto M, Kishimoto T, Akira S. Phosphorylation at threonine-235 by a ras-dependent mitogen-activated protein kinase cascade is essential for transcription factor NF-IL6. *Proc Natl Acad Sci U S A*. 1993;90(6):2207–11.
- Chien CM, Lin KL, Su JC, Chuang PW, Tseng CH, Chen YL, Chang LS, Lin SR. Naphtho[1,2-b]furan-4,5-dione induces apoptosis of oral squamous cell carcinoma: involvement of EGF receptor/PI3K/Akt signaling pathway. *Eur J Pharmacol*. 2010;636(1–3):52–8.
- Hennessy BT, Smith DL, Ram PT, Lu Y, Mills GB. Exploiting the PI3K/AKT pathway for cancer drug discovery. *Nat Rev Drug Discov*. 2005;4(12):988–1004.
- Kongtawelert P, Wuudtiwai B, Shwe TH, Pothacharoen P, Phitak T. Inhibitory effect of hesperidin on the expression of programmed death ligand (PD-L1) in breast cancer. *Molecules*. 2020;25(2):252.
- Zou W, Wolchok JD, Chen L. PD-L1 (B7-H1) and PD-1 pathway blockade for cancer therapy: mechanisms, response biomarkers, and combinations. *Sci Transl Med*. 2016;8(328):328–324.
- Dong H, Strome SE, Salomao DR, Tamura H, Hirano F, Flies DB, Roche PC, Lu J, Zhu G, Tamada K, et al. Tumor-associated B7-H1 promotes T-cell apoptosis: a potential mechanism of immune evasion. *Nat Med*. 2002;8(8):793–800.
- Cheng Y, Li H, Deng Y, Tai Y, Zeng K, Zhang Y, Liu W, Zhang Q, Yang Y. Cancer-associated fibroblasts induce PDL1+ neutrophils through the IL6-STAT3 pathway that foster immune suppression in hepatocellular carcinoma. *Cell Death Dis*. 2018;9(4):422.
- Planes-Laine G, Rochigneux P, Bertucci F, Chretien AS, Viens P, Sabatier R, Goncalves A. PD-1/PD-L1 targeting in breast cancer: the first clinical evidences are emerging. A literature review. *Cancers* (Basel). 2019;11(7):1033.

24. Jirapongwattana N, Thongchot S, Chiraphapphaiboon W, Chieochansin T, Sa-Nguanraksa D, Warnnissorn M, Thuwajit P, Yenchtsomanus PT, Thuwajit C. Mesothelin-specific T cell cytotoxicity against triple negative breast cancer is enhanced by 40s ribosomal protein subunit 3-treated self-differentiated dendritic cells. *Oncol Rep*. 2022;48(1):1–11.
25. Luangwattananun P, Junking M, Sujitjoo J, Wutti-In Y, Pongvarin N, Thuwajit C, Yenchtsomanus PT. Fourth-generation chimeric antigen receptor T cells targeting folate receptor alpha antigen expressed on breast cancer cells for adoptive T cell therapy. *Breast Cancer Res Treat*. 2021;186(1):25–36.
26. Cordes N, Winter N, Kolbe C, Kotter B, Mittelstaet J, Assenmacher M, Cathomen T, Kaiser A, Schaser T. Adapter-mediated transduction with lentiviral vectors: a novel tool for cell-type-specific gene transfer. *Viruses*. 2022;14(10):2157.
27. Su S, Chen J, Yao H, Liu J, Yu S, Lao L, Wang M, Luo M, Xing Y, Chen F, et al. CD10(+)/GPR77(+) cancer-associated fibroblasts promote cancer formation and chemoresistance by sustaining cancer stemness. *Cell*. 2018;172(4):841–56.
28. Calon A, Espinet E, Palomo-Ponce S, Tauriello DV, Iglesias M, Cespedes MV, Sevillano M, Nadal C, Jung P, Zhang XH, et al. Dependency of colorectal cancer on a TGF-beta-driven program in stromal cells for metastasis initiation. *Cancer Cell*. 2012;22(5):571–84.
29. Dittmer A, Lange T, Leyh B, Dittmer J. Protein- and growth-modulatory effects of carcinoma-associated fibroblasts on breast cancer cells: role of interleukin-6. *Int J Oncol*. 2020;56(1):258–72.
30. Liu H, Shen J, Lu K. IL-6 and PD-L1 blockade combination inhibits hepatocellular carcinoma cancer development in mouse model. *Biochem Biophys Res Commun*. 2017;486(2):239–44.
31. Feng R, Morine Y, Ikemoto T, Imura S, Iwahashi S, Saito Y, Shimada M. Nab-paclitaxel interrupts cancer-stromal interaction through C-X-C motif chemokine 10-mediated interleukin-6 downregulation in vitro. *Cancer Sci*. 2018;109(8):2509–19.
32. Cho H, Seo Y, Loke KM, Kim SW, Oh SM, Kim JH, Soh J, Kim HS, Lee H, Kim J, et al. Cancer-stimulated CAFs enhance monocyte differentiation and protumoral TAM activation via IL6 and GM-CSF secretion. *Clin Cancer Res*. 2018;24(21):5407–21.
33. Zhang R, Qi F, Zhao F, Li G, Shao S, Zhang X, Yuan L, Feng Y. Cancer-associated fibroblasts enhance tumor-associated macrophages enrichment and suppress NK cells function in colorectal cancer. *Cell Death Dis*. 2019;10(4):273.
34. Takahashi H, Sakakura K, Kawabata-Iwakawa R, Rokudai S, Toyoda M, Nishiyama M, Chikamatsu K. Immunosuppressive activity of cancer-associated fibroblasts in head and neck squamous cell carcinoma. *Cancer Immunol Immunother*. 2015;64(11):1407–17.
35. Liao D, Luo Y, Markowitz D, Xiang R, Reisfeld RA. Cancer associated fibroblasts promote tumor growth and metastasis by modulating the tumor immune microenvironment in a 4T1 murine breast cancer model. *PLoS ONE*. 2009;4(11): e7965.
36. Chen WJ, Ho CC, Chang YL, Chen HY, Lin CA, Ling TY, Yu SL, Yuan SS, Chen YJ, Lin CY, et al. Cancer-associated fibroblasts regulate the plasticity of lung cancer stemness via paracrine signalling. *Nat Commun*. 2014;5:3472.
37. Tong Y, Zhao Z, Zhang J, Wang W, Zhu Y. High expressions of CD10, FAP and GPR77 in CAFs are associated with chemoresistance and worse prognosis in gastric cancer. *Front Oncol*. 2022;12: 984817.
38. Heldin CH, Rubin K, Pietras K, Ostman A. High interstitial fluid pressure—an obstacle in cancer therapy. *Nat Rev Cancer*. 2004;4(10):806–13.
39. Fisher DT, Appenheimer MM, Evans SS. The two faces of IL-6 in the tumor microenvironment. *Semin Immunol*. 2014;26(1):38–47.
40. Manore SG, Doheny DL, Wong GL, Lo HW. IL-6/JAK/STAT3 signaling in breast cancer metastasis: biology and treatment. *Front Oncol*. 2022;12: 866014.
41. Iliopoulos D, Hirsch HA, Struhl K. An epigenetic switch involving NF-kappaB, Lin28, Let-7 MicroRNA, and IL6 links inflammation to cell transformation. *Cell*. 2009;139(4):693–706.
42. Mitchem JB, Brennan DJ, Knolhoff BL, Belt BA, Zhu Y, Sanford DE, Belaygorod L, Carpenter D, Collins L, Piwnica-Worms D, et al. Targeting tumor-infiltrating macrophages decreases tumor-initiating cells, relieves immunosuppression, and improves chemotherapeutic responses. *Cancer Res*. 2013;73(3):1128–41.
43. Burke WM, Jin X, Lin HJ, Huang M, Liu R, Reynolds RK, Lin J. Inhibition of constitutively active Stat3 suppresses growth of human ovarian and breast cancer cells. *Oncogene*. 2001;20(55):7925–34.
44. Lee HT, Xue J, Chou PC, Zhou A, Yang P, Conrad CA, Aldape KD, Priebe W, Patterson C, Sawaya R, et al. Stat3 orchestrates interaction between endothelial and tumor cells and inhibition of Stat3 suppresses brain metastasis of breast cancer cells. *Oncotarget*. 2015;6(12):10016–29.
45. Grivennikov S, Karin M. Autocrine IL-6 signaling: a key event in tumorigenesis? *Cancer Cell*. 2008;13(1):7–9.
46. Rose-John S, Jenkins BJ, Garbers C, Moll JM, Scheller J. Targeting IL-6 trans-signalling: past, present and future prospects. *Nat Rev Immunol*. 2023;28:1–16.
47. Cui C, Yu B, Jiang Q, Li X, Shi K, Yang Z. The roles of PD-1/PD-L1 and its signalling pathway in gastrointestinal tract cancers. *Clin Exp Pharmacol Physiol*. 2019;46(1):3–10.
48. Atsaves V, Tsesmetzis N, Chioureas D, Kis L, Leventaki V, Drakos E, Panaretakis T, Grandier D, Medeiros LJ, Young KH, et al. PD-L1 is commonly expressed and transcriptionally regulated by STAT3 and MYC in ALK-negative anaplastic large-cell lymphoma. *Leukemia*. 2017;31(7):1633–7.
49. Sasidharan Nair V, Toor SM, Ali BR, Elkord E. Dual inhibition of STAT1 and STAT3 activation downregulates expression of PD-L1 in human breast cancer cells. *Expert Opin Ther Targets*. 2018;22(6):547–57.
50. Zhang N, Zeng Y, Du W, Zhu J, Shen D, Liu Z, Huang JA. The EGFR pathway is involved in the regulation of PD-L1 expression via the IL-6/JAK/STAT3 signaling pathway in EGFR-mutated non-small cell lung cancer. *Int J Oncol*. 2016;49(4):1360–8.
51. Bu LL, Yu GT, Wu L, Mao L, Deng WW, Liu JF, Kulkarni AB, Zhang WF, Zhang L, Sun ZJ. STAT3 induces immunosuppression by upregulating PD-1/PD-L1 in HNSCC. *J Dent Res*. 2017;96(9):1027–34.
52. Johnson DE, O'Keefe RA, Grandis JR. Targeting the IL-6/JAK/STAT3 signalling axis in cancer. *Nat Rev Clin Oncol*. 2018;15(4):234–48.
53. Vasiyani H, Mane M, Rana K, Shinde A, Roy M, Singh J, Gohel D, Currim F, Srivastava R, Singh R. DNA damage induces STING mediated IL-6-STAT3 survival pathway in triple-negative breast cancer cells and decreased survival of breast cancer patients. *Apoptosis*. 2022;27(11–12):961–78.
54. Rodier F, Coppe JP, Patil CK, Hoeijmakers WA, Munoz DP, Raza SR, Freund A, Campeau E, Davalos AR, Campisi J. Persistent DNA damage signalling triggers senescence-associated inflammatory cytokine secretion. *Nat Cell Biol*. 2009;11(8):973–9.
55. Centurione L, Aiello FB. DNA repair and cytokines: TGF-beta, IL-6, and thrombopoietin as different biomarkers of radioresistance. *Front Oncol*. 2016;6:175.
56. Sherman MH, Yu RT, Engle DD, Ding N, Atkins AR, Tiriach H, Collisson EA, Connor F, Van Dyke T, Kozlov S, et al. Vitamin D receptor-mediated stromal reprogramming suppresses pancreatitis and enhances pancreatic cancer therapy. *Cell*. 2014;159(1):80–93.
57. Ding N, Yu RT, Subramaniam N, Sherman MH, Wilson C, Rao R, Leblanc M, Coulter S, He M, Scott C, et al. A vitamin D receptor/SMAD genomic circuit gates hepatic fibrotic response. *Cell*. 2013;153(3):601–13.
58. Sarker M, Cortes E, Lieberthal TJ, Del Rio HA. ATRA modulates mechanical activation of TGF-beta by pancreatic stellate cells. *Sci Rep*. 2016;6:27639.
59. Korkaya H, Kim GI, Davis A, Malik F, Henry NL, Ithimakin S, Quraishi AA, Tawakkol N, D'Angelo R, Paulson AK, et al. Activation of an IL6 inflammatory loop mediates trastuzumab resistance in HER2+ breast cancer by expanding the cancer stem cell population. *Mol Cell*. 2012;47(4):570–84.
60. Hu Y, Yague E, Zhao J, Wang L, Bai J, Yang Q, Pan T, Zhao H, Liu J, Zhang J. Sabutoclax, pan-active BCL-2 protein family antagonist, overcomes drug resistance and eliminates cancer stem cells in breast cancer. *Cancer Lett*. 2018;423:47–59.
61. Tu B, Zhu J, Liu S, Wang L, Fan Q, Hao Y, Fan C, Tang TT. Mesenchymal stem cells promote osteosarcoma cell survival and drug resistance through activation of STAT3. *Oncotarget*. 2016;7(30):48296–308.
62. Mace TA, Shakya R, Pitarresi JR, Swanson B, McQuinn CW, Loftus S, Nordquist E, Cruz-Monserrate Z, Yu L, Young G, et al. IL-6 and PD-L1 antibody blockade combination therapy reduces tumour progression in murine models of pancreatic cancer. *Gut*. 2018;67(2):320–32.

63. Liu Y, Zhou Y, Huang KH, Li Y, Fang X, An L, Wang F, Chen Q, Zhang Y, Shi A, et al. EGFR-specific CAR-T cells trigger cell lysis in EGFR-positive TNBC. *Aging (Albany NY)*. 2019;11(23):11054–72.
64. Liu Y, Lian T, Yao Y. A systematic review and meta-analysis of higher expression of folate receptor alpha (FOLR1) predicts poor cancer prognosis. *Biomarkers*. 2020;25(5):367–74.
65. Lin J, Spidel JL, Maddage CJ, Rybinski KA, Kennedy RP, Krauthauser CL, Park YC, Albone EF, Jacob S, Goserud MT, et al. The antitumor activity of the human FOLR1-specific monoclonal antibody, farletuzumab, in an ovarian cancer mouse model is mediated by antibody-dependent cellular cytotoxicity. *Cancer Biol Ther*. 2013;14(11):1032–8.
66. Farran B, Pavitra E, Kasa P, Peela S, Rama Raju GS, Nagaraju GP. Folate-targeted immunotherapies: passive and active strategies for cancer. *Cytokine Growth Factor Rev*. 2019;45:45–52.
67. O'Shannessy DJ, Somers EB, Maltzman J, Smale R, Fu YS. Folate receptor alpha (FRA) expression in breast cancer: identification of a new molecular subtype and association with triple negative disease. *Springerplus*. 2012;1:22.
68. Feig C, Jones JO, Kraman M, Wells RJ, Deonaraine A, Chan DS, Connell CM, Roberts EW, Zhao Q, Caballero OL, et al. Targeting CXCL12 from FAP-expressing carcinoma-associated fibroblasts synergizes with anti-PD-L1 immunotherapy in pancreatic cancer. *Proc Natl Acad Sci U S A*. 2013;110(50):20212–7.

### Publisher's Note

Springer Nature remains neutral with regard to jurisdictional claims in published maps and institutional affiliations.

Ready to submit your research? Choose BMC and benefit from:

- fast, convenient online submission
- thorough peer review by experienced researchers in your field
- rapid publication on acceptance
- support for research data, including large and complex data types
- gold Open Access which fosters wider collaboration and increased citations
- maximum visibility for your research: over 100M website views per year

At BMC, research is always in progress.

Learn more [biomedcentral.com/submissions](https://biomedcentral.com/submissions)

